

CALCULATION OF A MODEL FOR THE ELECTRON FERMI SURFACE IN INDIUM

M. E. ARUSTAMOVA, R. T. MINA, and V. S. POGOSYAN

Erevan Physics Institute

Submitted December 10, 1968

Zh. Eksp. Teor. Fiz. 56, 1983–1991 (June, 1969)

A ‘‘Razdan-3’’ electronic computer is employed to set up, in the approximation of three orthogonal plane waves,^[13] a model of the β tube of the electron Fermi surface in indium. The single-parameter pseudopotential model proposed by Harrison^[13] is used. For each value of the parameter β , the computer yielded a value of the Fermi energy such that the corresponding area of the tube cross section was equal to that measured experimentally on basis of the de Haas–van Alphen effect^[1]. Additional experimental data on the size effect^[4,7] were used to determine the pseudopotential and Fermi energy and to set up a model of the electron surface. The anisotropy in the $(1\bar{1}0)$ plane, the cross section area of the tube, the extremal size, and the effective mass are calculated for this model and are compared with experiment^[1,4,6]. The calculated dependence of the model parameters on the experimentally-measured quantities^[2,4] permit an estimate of the degree of indeterminacy of the parameters and to select the experimental results that are most important for the model.

RECENT intense experimental investigations of the energy spectrum of electrons in indium^[1–11] have made it possible to attempt^[6,8,10,12] to construct a model of its Fermi surface. According to the concepts that have developed to date, the almost-free electron approximation is valid for a large number of polyvalent metals. In this approximation, the action of the crystal lattice field on the carrier motion can be taken into account by introducing a weak effective pseudopotential^[13]. This pseudopotential was calculated^[12] with the aid of atomic wave functions of the electrons of an isolated ion. However, the correspondingly constructed model of the Fermi surface turned out to contradict the experimental results^[3,4,6,9,11].

A different method was used in a number of papers^[6,8,10], wherein the pseudopotential was chosen such as to make the corresponding Fermi-surface model agree best with the experimental results that are most sensitive to its magnitude. The effectiveness of this method is enhanced also by the fact that the qualitative character of the pseudopotential is known and can be specified for many polyvalent metals by means of an approximate formula with only one unknown parameter.^[13,14]

Table I lists the results of^[6,8,10,12]. We see that although the results of^[6,8,10] are qualitatively more or less in agreement with one another with respect to the signs and proportionality of the corresponding quantities, there is no complete quantitative agreement. The reason lies apparently in the fact that in order to choose the pseudopotential, a limited amount of experimental data was used in each case. Therefore, for example, in

all these calculations, the Fermi energy of the carriers was assumed equal to the energy of the free electrons.

In the present paper, just as in^[8], we determine the pseudopotential by using the value of the smallest reliably known cross section of the β tube of the third-zone electronic Fermi surface. However, unlike in^[8], the modified value of the Fermi energy of the electrons has made it possible to reconcile the size-effect data^[4] with the Fermi-surface model. The calculation program was made up in such a way as to take into account the possible errors connected with the inaccuracy of the employed experimental values. The results of our calculations are also contained in Table I. For the obtained values of the pseudopotential and the Fermi energy, we calculated the anisotropy in the (110) plane of the cross-section area of the tube, of the extremal size, and of the effective mass, and compared the results with the experimental data^[1,4,6].

CALCULATION

1. The crystal lattice of indium can be represented as a tetragonal face-centered lattice with axis ratio $c' = a/c = 0.9243$, $c = 4.904 \text{ \AA}$, and $a = 4.532 \text{ \AA}$ at $T = 0^\circ \text{K}$. These values were obtained by extrapolating to absolute zero the measurements made in^[15] between room and nitrogen temperatures. Since the valence of indium is $z = 3$, it follows that in accordance with the free-electron model (the 1-OPW model), the radius of the Fermi surface $p_{FC} = 1.10 h/a$, and the Fermi energy is $E_{FC} = p_{FC}^2/2m_c = 1.21 (h/a)^2/2m_c = 0.6516 \text{ Ry}$ (the latter equality is valid if the carrier mass m_c is equal to the electron mass m_e).

2. According to the 1-OPW model, the electron Fermi surface of indium in the third zone consists of four identical β tubes joined end to end^[1]. Each tube is made up of an intersection of three Fermi surfaces. Figure 1 shows the intersection of one of the tubes with the (110) plane. The centers $(0, 0, 0)$, $(1, 1, 1)$, and $(1, 1, -1)$ of the corresponding Fermi spheres, located in the sites of the reciprocal lattices, have in the figure the coordinates $(0, 0, 0)$, $(\sqrt{2}, c', 0)$, and $(\sqrt{2}, -c', 0)$.

Table I

Component of pseudopotential $V, (h/a)^2/2m_c$			$E_F, (h/a)^2/2m_c$	Reference
$V_{[111]}$	$V_{[002]}$	$V_{[200]}$		
-0.07 ± 0.015	-0.055 ± 0.01	0.00 ± 0.015	1.21	[5]
-0.087	-0.037	0.00	1.21	[8]
-0.093	-0.058	$+0.0013$	1.21	[10]
-0.01523	-0.0186	$+0.049$	1.17	[12]
-0.136 ± 0.020	-0.085 ± 0.020	-0.046 ± 0.020	1.247 ± 0.019	Present work

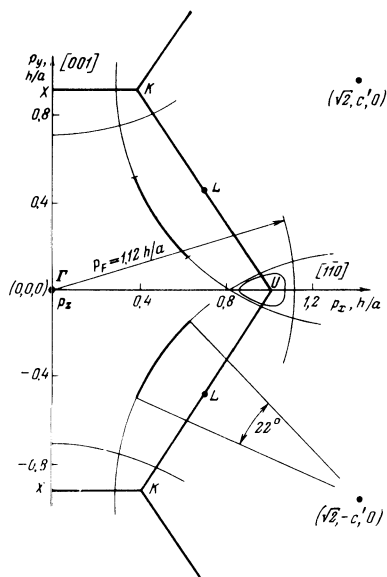


FIG. 1. Intersection of the (110) plane and the Fermi surface of indium: model 1-OPW ($p_F = 1.117h/a$)—thin lines, model 3-OPW ($V_{1111} = -0.136$, $V_{1002} = 0.085$, $E_F = 1.247$ in units of $(h/a)^2/2m_c$)—thick line. Straight lines—intersection of the faces of the Brillouin zone with the (110) plane.

The free-electron energy E_C at the point U (Fig. 1), which is equidistant from all three centers, has three-fold degeneracy, which is lifted by the lattice pseudopotential V. According to perturbation theory, the new values of the energy in the vicinity of the point U are determined by the secular equation

$$\begin{vmatrix} p_x^2 + p_y^2 + 2m_c V_1 & 2m_c V_1 \\ + p_z^2 - 2m_c E & (p_x - \sqrt{2})^2 + (p_y - c')^2 + 2m_c V_2 \\ 2m_c V_1 & + p_z^2 - 2m_c E \\ 2m_c V_1 & (p_x - \sqrt{2})^2 + (p_y + c')^2 + 2m_c V_2 \\ & + p_z^2 - 2m_c E \end{vmatrix} = 0, \quad (1)$$

where V_1 and V_2 denote, for brevity, the lattice pseudopotential Fourier components^[13] along the axes $[111]$ and $[002]$, and p_x , p_y , and p_z are the components of the electron momentum \mathbf{p} in the coordinate system of Fig. 1.

The aggregate of the points for which Eq. (1) is valid forms at $E = E_F$ the 3-OPW model of the Fermi-surface tube β ^[13].

4. As shown by calculations of the pseudopotential of many polyvalent metals, it can be satisfactorily approximated by a function dependent only on a single parameter β ^[13]:

$$V_p = -\frac{Ze^2 h^2 / \pi p^2 + \beta}{\Omega_0 \epsilon(p)}, \quad (2)$$

where

$$\epsilon(p) = 1 + \frac{m_e^2}{2\pi p_F \hbar \eta^2} \left(\frac{1 - \eta^2}{2\eta} \ln \left| \frac{1 + \eta}{1 - \eta} \right| + 1 \right)$$

is the dielectric constant of the free electrons in the Hartree approximation ($\eta = p/2p_F$), and Ω_0 is the atomic volume. The dimension of the parameter β is $\text{Ry} \cdot (\text{at. un.})^3$ and will henceforth be omitted for brevity.

5. The calculations were performed with the "Razdan-3" computer in several stages. For a specified parameter β and for $E = E_F$, formula (2) was used

to determine the components $V_1(\beta, E)$ and $V_2(\beta, E)$. By solving Eq. (1) in the plane (110), we obtained more than 200 points (p_x, p_y) lying on the contour of the tube section. The cross section area calculated with accuracy 10^{-3} was compared with the experimental value $S_0 = 0.02294 (h/a)^2$, which was introduced into the program. Depending on the sign and magnitude of the difference of the areas, the magnitude of the energy E was changed to bring it closer to the final result, and the new value of the energy E was used to repeat the entire preceding cycle of the calculations. After approximately 10 cycles, the area of the calculated cross section became equal to the experimental area, and a printout was obtained for the coordinates of all the points (p_x, p_y) of the cross section contour, for the energy, and for the components of the pseudopotential. At the same time, the value of the effective mass was determined from the formula

$$m^* = \frac{1}{2\pi} \frac{dS}{dE} \Big|_{E=E_F} \quad (3)$$

The foregoing calculation program was executed for eight values of the parameter β in the interval $30 \leq \beta \leq 37$. The results of the calculations for $S_0 = 0.02294 (h/a)^2$ are shown in Figs. 2–4. The values of the pseudopotential components and of the Fermi energy corresponding to $\beta = 30$ are contained in Table I. The form of the intersection of the tube in accordance with the 3-OPW model with the (110) plane is shown in Fig. 5 for three different values of the parameter β .

6. For values of the parameter $\beta = 30$ and $S_0 = 0.02294 (h/a)^2$, we calculated the anisotropy of the area of the tube sections in the $(1\bar{1}0)$ plane, the extremal

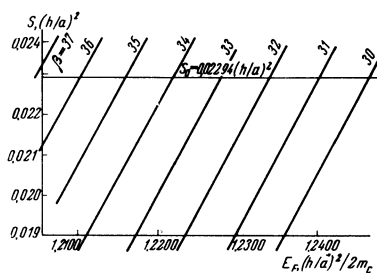


FIG. 2. Plots of the cross section area S of the β tube against the Fermi energy E_F for different values of the parameter β .

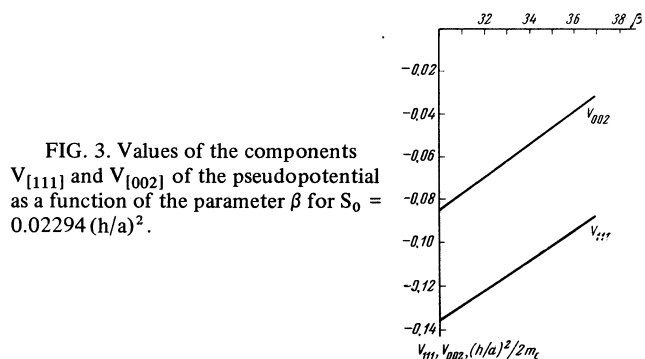


FIG. 3. Values of the components V_{1111} and V_{1002} of the pseudopotential as a function of the parameter β for $S_0 = 0.02294 (h/a)^2$.

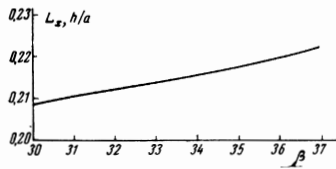


FIG. 4. Dependence of the extremal dimension L along the $[\bar{1}\bar{1}0]$ axis (x axis in Fig. 1) on the parameter β for $S_0 = 0.02294 (h/a)^2$.

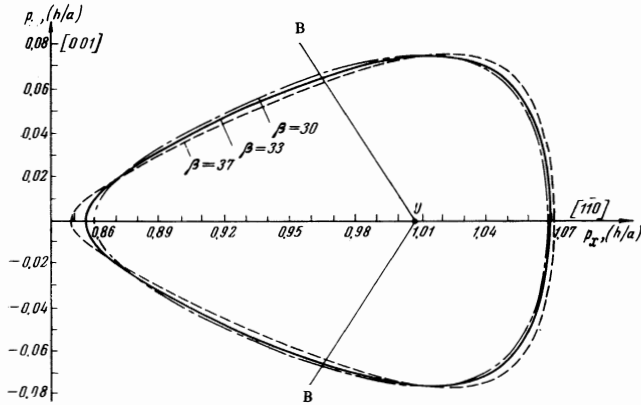


FIG. 5. Intersections of the β tube of the 3-OPW model with the (110) plane for three values of the parameter β having the same area $S_0 = 0.02294 (h/a)^2$. The straight lines B and the point U are the intersection of the faces of the Brillouin zone with the (110) plane.

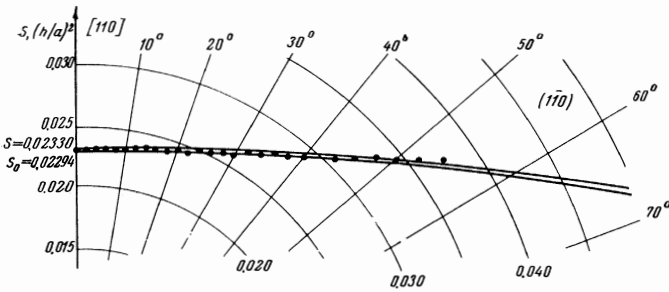


FIG. 6. Anisotropy of the area of the central section of the tube β in the $(\bar{1}\bar{1}0)$ plane. Solid lines—results of calculations for values of the parameter $\beta = 30$ and two values of the area, $S_0 = 0.02330 (h/a)^2$ and $S_0 = 0.02294 (h/a)^2$, at $H \parallel [110]$; points—experimental data of Fig. 4 of [2]

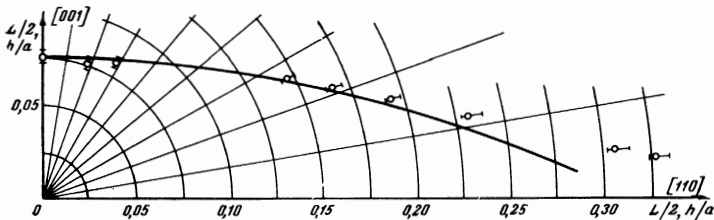


FIG. 7. Anisotropy of the experimental dimension of tube β in the $(\bar{1}\bar{1}0)$ plane). Solid line—result of the calculation for the values of the parameter $\beta = 30$ and the area $S_0 = 0.02294 (h/a)^2$; points with the indicated measurement error—experimental data of [4].

dimension (in a direction orthogonal to $[\bar{1}\bar{1}0]$, i.e., the abscissa axis in Fig. 1), and the effective mass μ . To determine the latter, we performed additional calculations of the cross section area anisotropy at the same value of the parameter β and for $S = 0.02330 (h/a)^2$. All these data are shown in Figs. 6–8.

7. The calculation accuracy of the 3-OPW tube model depends on the accuracy of the initial experimental values, namely the cross section area S and one of the extremal dimensions L , for example the one parallel to $[\bar{1}\bar{1}0]$. For this reason the program for the calculations and for the readout of the intermediate results from the computer was compiled in such a way as to take into account the inaccuracy of the experimental data. It is easy to show that a small change in any calculated quantity A is connected with changes of S and L in the following manner:

$$\Delta A = \left(\frac{\partial A}{\partial \beta} \middle| \frac{\partial L}{\partial \beta} \right)_s \Delta L + \left\{ \left(\frac{\partial A}{\partial S} \right)_\beta - \left(\frac{\partial A}{\partial \beta} \middle| \frac{\partial L}{\partial \beta} \right)_s \left(\frac{\partial L}{\partial S} \right)_\beta \right\} \Delta S. \quad (4)$$

If A is taken to mean the parameter β , formula (4) takes the simpler form

$$\Delta \beta = \frac{\Delta L + (\partial L / \partial S)_\beta \Delta S}{(\partial L / \partial \beta)_s}. \quad (5)$$

COMPARISON OF CALCULATION WITH THE EXPERIMENTAL RESULTS

1. Table II lists the extremal dimensions L of the sections of the 3-OPW model tube for $\beta = 30$ and those measured in [4]1). The good agreement between them offers evidence that the shape of the sample section of the tube in the (110) plane agrees with the 3-OPW model. A comparison of the anisotropy in the (110) plane of the section area and of the extremal dimension, calculated in accordance with this model, with the experimental data of [1,4] is shown in Figs. 6 and 7. Up to an approximate angle 60° between H and $[\bar{1}\bar{1}0]$, the experiment agrees with the calculation within the limits of errors. At larger angles, the anisotropy of the extremal dimension differs noticeably from the calculated anisotropy. This difference results from the fact that the 3-OPW model, which is valid for sections of the Fermi surface near the point U , ceases to represent correctly the singularities of the electronic Fermi surface near the points where the tubes are joined, at which the orbit falls at angles $\geq 60^\circ$ between H and $[\bar{1}\bar{1}0]$.

2. A comparison of the calculated effective mass

Table II

$\chi(L; [\bar{1}\bar{1}0])$ in the (110) plane, deg	Extremal dimension L, h/a		$(dL/d\beta)_s,$ h/a per unit of β
	Measured in [4]	Calculated for $\beta = 30, S = 0.02294$	
0	0.207 ± 0.005	0.2084	0.00193
24	0.200 ± 0.005	0.2026	0.00193
56	0.171 ± 0.005	0.1703	0.00080
90	0.150 ± 0.005	0.1503	0.00025

1)The authors are grateful to I. P. Krylov for supplying the table of the measurement results of [4] calculated in accordance with the conclusions of [7].

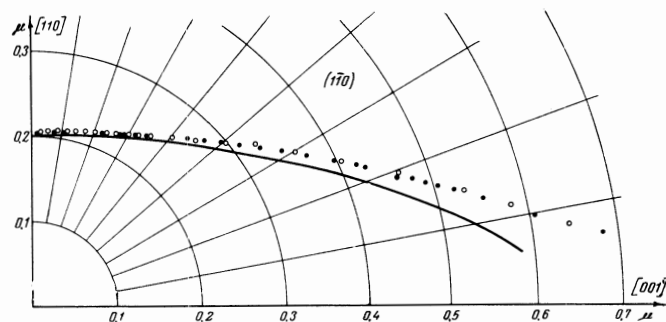


FIG. 8. Anisotropy of effective mass in the (110) plane. The solid line was calculated with the aid of the data of Fig. 6 for the values of the parameter $\beta = 30$ and the area $S_0 = 0.02294(h/a)^2$ and $m_C = 1.65m_e$. The symbols \circ and \bullet represent the data of Fig. 11 of [6].

corresponding to the section of the tube with the volume measured experimentally by cyclotron resonance is shown in Fig. 8.

The effective mass m^* calculated by means of formula (3) is directly proportional to the mass m_C of the carrier in the metal. This fact follows directly from the energy dimension. For almost all the metals, m_C differs greatly from the electron mass m_e . This circumstance is due to the existence of electron-phonon interaction^[13]. In^[5,6] it was shown experimentally that $m_C = 1.6m_e$ for the hole Fermi surface. In^[6], for the electron Fermi surface, the proportionality coefficient was estimated at ~ 1.4 . This approximate estimate was obtained on the basis of the information given in^[4] concerning the perimeter of the tube cross section. Our results make it possible to obtain these coefficients much more accurately. This is due to the fact that the effective mass was calculated with the aid of the 3-OPW model surface, the shape of which, as already shown, is quite close to the real tube surface. The calculated effective mass $m^* = 0.122m_C$ becomes equal to the measured value $\mu = m^*/m_e = 0.202$ ^[6], if it is assumed that $m_C = 1.65m_e$. This proportionality coefficient is somewhat larger than that obtained experimentally for the hole surface, but is quite close to it. It is interesting to note that for aluminum, the Fermi surface of which is similar to the Fermi surface of indium, the inverse relation holds true. For the hole surface $m_C = 1.55m_e$ ^[16], and for the electron surface $m_C = 1.4m_e$ ^[17].

3. The effective-mass anisotropy calculated under the assumption $m_C = 1.65m_e$, is compared in Fig. 8 with the anisotropy measured in the experiments of^[6]. The noticeable difference between them can be due to the inaccuracy of the 3-OPW model, which comes into play at large angles between H and $[110]$, in analogy with the situation for the extremal-dimensional anisotropy (Fig. 7). In this case, however, unlike in the latter case, the different anisotropy can be qualitatively attributed to the decrease of m_C on the surface of the tube, from the center towards its edges. A quantitative comparison can be carried out only by performing the calculations on the basis of the more accurate 4-OPW model.

4. The results of the calculations indicate which of the size-effect measurement data are the most valuable for the calculation of the Fermi surface of the tube. It is seen from Fig. 5, that given the tube cross section

area, the extremal dimensions of the tube cross section along the different directions L change in different manners when the parameter β is varied.

A separate column in Table II indicates the derivatives $(\partial L_i/\partial \beta)_S$ for four different directions of L . Their value shows that the dimension along $[1\bar{1}0]$ is most sensitive to the change of the parameter β , whereas the sensitivity of the dimension along $[001]$ is lower by one order of magnitude.

5. The inaccuracy of the experimental data limits the calculation capabilities of the 3-OPW model. The probable calculation errors can be determined from formula (4). To estimate the absolute calculation error, it is necessary to know the accuracy of the experimental data. The value of the extremal dimension along $[1\bar{1}0]$ and the accuracy of its determination are listed in Table II. Unfortunately, there are no estimates of the error ΔS_0 of the measurement of the cross section area S_0 in^[11]. From Table I of that paper one can conclude that $\Delta S_0/S_0 = 1\%$, since three different values of the area, ascribed to $H \parallel [110]$, fall in this interval. However, the spread of the experimental points is smaller, and amounts to $\sim 0.4\%$. This gives grounds for assuming that the difference in the tabulated values of S_0 is due to inaccuracy in the crystallographic orientation of the samples, equal to $\sim 0.5^\circ$. For this reason, we used in the present calculations the smallest of the numbers S_0 from Table I of^[11].

The substitutions

$$S_0 = 0.02294(h/a)^2, L = 0.21h/a, \Delta S_0 = \pm 0.0001(h/a)^2$$

and $\Delta L \pm 0.005h/a$ in formulas (4) makes it possible to determine the following calculation errors:

$$\begin{aligned} \Delta\beta &= 110 \frac{\Delta L}{L} + 54.0 \frac{\Delta S}{S} = \pm 2.60 \pm 0.24 \approx \pm 3, \\ \Delta V &= -0.81 \frac{\Delta L}{L} + 0.38 \frac{\Delta S}{S} = \pm 0.018 \pm 0.002 \approx \pm 0.02, \\ \Delta E_F &= -0.73 \frac{\Delta L}{L} + 0.40 \frac{\Delta S}{S} = \pm 0.017 \pm 0.0017 \approx \pm 0.019, \end{aligned} \quad (6)$$

some of which are listed in Table I. $\Delta\beta$ is given in units of $Ry \cdot (\text{at.un.})^3$, and ΔV and ΔE_F in units of $(h/a)^2/2m_C$.

It follows from (6) that the contribution to the total error of the calculation of the pseudopotential and of the Fermi energy is smaller for the de Haas-van Alphen effect than for the size effect.

From the Fermi energy calculated in this paper (Table I) it follows that the radius of the Fermi sphere is $p_F = (1.117 \pm 0.008)h/a$. This value was used in constructing the 1-OPW model of the tube cross section in Fig. 1.

The Gaussian curvature of the part of the hole Fermi surface of the second zone was determined in^[7]. Its central section, shown by the heavy line on the (110) section of the 1-OPW model (Fig. 1), has a constant curvature within the limits of the experimental accuracy. It is therefore not distorted by the presence of the pseudopotential, and constitutes a sphere of radius $p_F = (1.11 \pm 0.02)h/a$. The calculated value coincides with the measured one within the limits of errors.

In conclusion, the authors consider it their pleasant duty to thank A. I. Alikhanyan for interest in the work, and I. P. Krylov and K. Sh. Agababyan for a useful discussion and for remarks.

- ¹J. A. Rayne, Phys. Rev. **129**, 652 (1962).
- ²G. B. Brandt and J. A. Rayne, Phys. Rev. **132**, 1512 (1963).
- ³Yu. P. Gaĭdukov, Zh. Eksp. Teor. Fiz. **49**, 1049 (1965) [Sov. Phys.-JETP **22**, 730 (1966)].
- ⁴V. F. Gantmakher and I. P. Krylov, Zh. Eksp. Teor. Fiz. **49**, 1054 (1965) [Sov. Phys.-JETP **22**, 734 (1966)].
- ⁵R. T. Mina and M. S. Khaĭkin, ZhETF Pis. Red. **1**, No. 2, 34 (1965) [JETP Lett. **1**, 60 (1965)].
- ⁶R. T. Mina and M. S. Khaĭkin, Zh. Eksp. Teor. Fiz. **51**, 62 (1966) [Sov. Phys.-JETP **24**, 42 (1967)].
- ⁷I. P. Krylov and V. F. Gantmakher, Zh. Eksp. Teor. Fiz. **51**, 740 (1966) [Sov. Phys.-JETP **24**, 492 (1967)].
- ⁸W. J. O'Sullivan, J. E. Schirber, and J. R. Anderson, Solid State Comm. **5**, 525 (1967).
- ⁹R. Koyama, W. E. Spicer, N. W. Ashcroft, and W. E. Lawrence, Phys. Rev. Lett. **19**, 1284 (1967).
- ¹⁰W. J. O'Sullivan, J. E. Schirber, and J. R. Anderson, Phys. Lett. **27A**, 144 (1968).
- ¹¹A. J. Haghes and A. H. Lettington, Phys. Lett. **27A**, 241 (1968).
- ¹²G. D. Gaspari, W. E. Spicer, and T. P. Das, Phys. Rev. **167**, 660 (1968).
- ¹³W. Harrison, Pseudopotentials in the Theory of Metals, Benjamin, 1966.
- ¹⁴N. W. Ashcroft, Phys. Lett. **23**, 48 (1966).
- ¹⁵J. Graham, A. Moore, and G. V. Raynov, J. Inst. Metals **84**, 86 (1965).
- ¹⁶F. W. Spong, and A. F. Kip, Phys. Rev. **137A**, 431 (1965).
- ¹⁷G. O. Larson and W. L. Gordon, Phys. Rev. **156**, 703 (1967).

Translated by J. G. Adashko
230